

EE412 Spring 2015 Final Report

Vertical Semiconductor Blades

Martin Winterkorn, Anup Dadlani, Karen Kim

Mentor: J Provine

1. Motivation and Overview

The goal of this project was to develop and characterize the key fabrication steps for a new high-throughput process – as an alternative to focused ion beam (FIB) patterning – to manufacture narrow, high-aspect ratio blades of the III-V materials InSb or InAs. Ideally a width of 50 nm and an aspect ratio of 10:1 for several um long isolated, sparse blades should be achievable. The key steps were identified as the deposition of the III-V material, the lithography and the patterning of the III-V layer by reactive ion etching (RIE).

For deposition, two options were considered: RF magnetron sputtering of InSb or MOCVD of InAs. The InSb sputtering is a capability previously developed in our own lab and therefore not the main focus of the project. MOCVD of InAs is possible in the new MOCVD lab that is part of SNF, however heterogeneous growth of thick InAs films has not been extensively characterized, hence this is the first main area we wanted to explore.

In terms of lithography, the most common way to achieve feature sizes below the wavelength of standard optical lithography is by using e-beam lithography, for which there are two machines available at Stanford, the Raith at SNF and the newer JEOL in the Nanopatterning Cleanroom at SNSF. However, despite them being heavily booked tools, compared to optical lithography there is very little information publicly available about the various steps of the e-beam process, such as properties of different resists, coating recipes, exposure dosages etc., and even less about integration with SNF processes such as resist etch rates. The goal for our exploration of e-beam using the JEOL in SNC was therefore to focus on these factors and to compile information that would help labmembers who are new to e-beam or just considering the process, like ourselves.

One big advantage of e-beam in regards to our overall fabrication goal is that due to its high resolution, achieving the 50 nm width target for the lines would not be a challenge. However, there are also significant disadvantages compared to optical lithography, such as very long write times and subsequently low throughput, as well as high cost and worse fab integration in SNF. Especially the sequential nature of e-beam is somewhat counter to one of the goals of the project, namely to replace a slow sequential process (FIB). Therefore, in parallel an effort was made to achieve 50 nm isolated lines with optical lithography by using double exposure methods.

Double exposure is a widely known technique to achieve feature sizes below the traditional resolution limit, but it has not been extensively tested or characterized on the i-line ASML stepper in SNF. While it certainly will not be able to replace e-beam in many cases, there are several applications, e.g. thermal actuators or sensors, which like ours simply require very thin lines instead of complex geometries, so that double exposure would be very attractive to a wide range of labmembers if it turns out to be feasible.

Finally, to be able to transfer the lithographic patterns onto the semiconductor material and fabricate the blades, a new etch had to be developed. With the Oxford-III-V etcher, there is a tool available at SNF dedicated for III-V-materials etching, but there were no recipes available for either InAs or InSb etching. For the reasons described in the MOCVD section, we focused on InSb. After literature review we explored the recipe parameter space using a design-of-experiment (DOE) approach, while aiming to optimize for our particular requirements such as vertical and smooth sidewalls.

2. Heterogeneous InAs MOCVD growth

The architecture of our final devices requires the III-V film to be grown on a single crystal Si substrate. The high lattice mismatch between Si and InAs makes this challenging, leading to significant tradeoffs between crystal quality, surface roughness and deposition rate. Depositions at lower temperatures are expected to have better i.e. lower surface roughness, but smaller grain sizes and lower deposition rate, whereas higher temperature deposition improves those two parameters at the expense of more roughness and worse uniformity.

With 50 nm blade width and 10:1 aspect ratio, a film thickness of at least 500 nm was required. This effectively puts a lower limit on the temperature, since going too low would reduce the deposition rate so much to make the process not feasible, especially considering the expense of the precursors. With this in mind, two test depositions were carried out at 400C and 500C. Characterization was done using 3D optical profilometry, XRD and TEM.

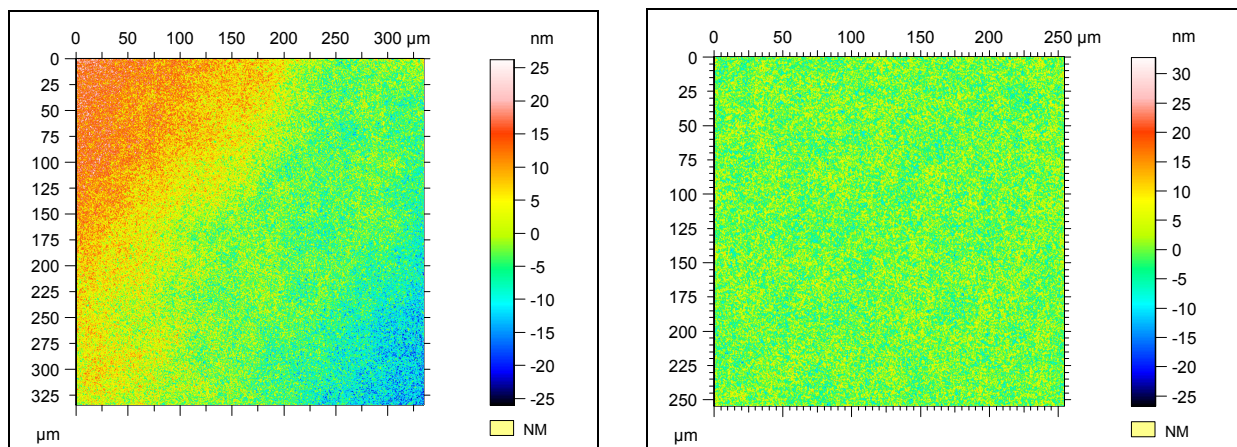


Figure 1. CCI-HD measurement of MOVCD-grown InAs, with waviness filtered out (right).

The first surface roughness measurements (Figure 1), taken with the CCI-HD optical 3D profilometer in SNF were promising, showing an RMS roughness of only 4.3 nm. However when doing TEM characterization (Figure 2), it turned out that these numbers were severely underestimating the actual roughness. This likely explanation for this is that despite the CCI-HD's high vertical resolution on the order of 0.1 nm, the low lateral resolution around 1 μm is too coarse to follow the actual steps. The actual surface roughness from TEM is estimated to be on the order of 50 nm for the 400 C case.

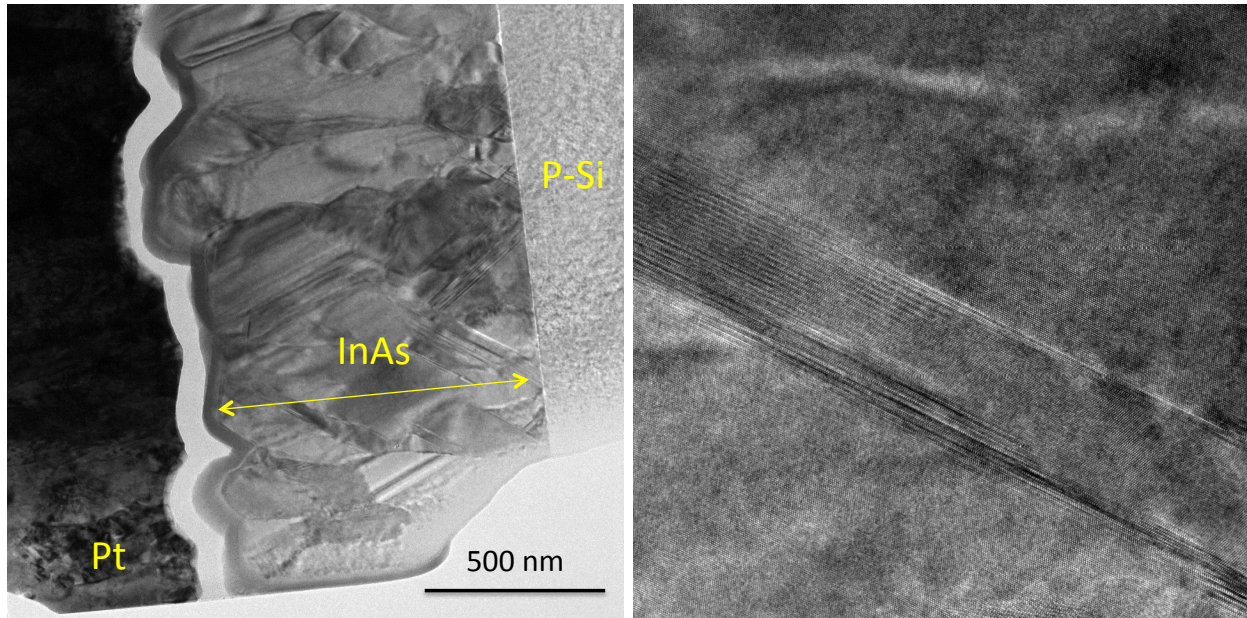


Figure 2. TEM characterization of MOVCD-grown InAs.

The TEM images also show fairly small crystal sizes and many defects such as stacking faults (right). The XRD results (Figure 3) confirm the crystalline morphology. Overall, it was quickly determined that without significant efforts in recipe development or annealing, MOCVD would not be a viable option for our devices and due to the anticipated time constraints of the project, the decision was made to focus on sputtered InSb as the basis for the other parts.

3. ASML Double Exposures

The main principle of double exposure is to take advantage of the fact that the typical error in the alignment between two different exposure shots, as specified by the standard deviation in nm, is significantly lower than the thinnest line that can be exposed as limited by diffraction.

3.1 Single Resist Double Exposure

The way to use this that would integrate most easily into any fabrication process is by exposing a single layer of resist twice, as illustrated in Figure 4. Exposing an image that leaves a line with a

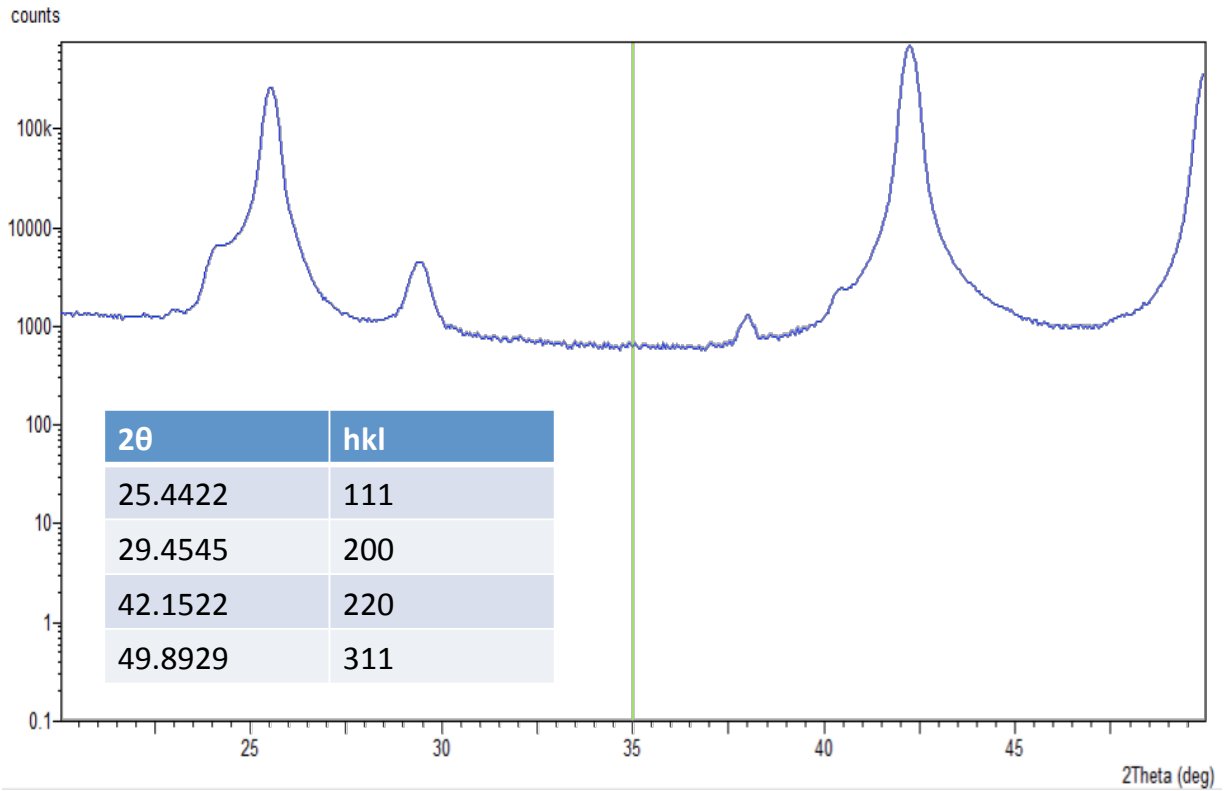


Figure 3. XRD measurement of MOVCD-grown InAs with corresponding crystal orientations.

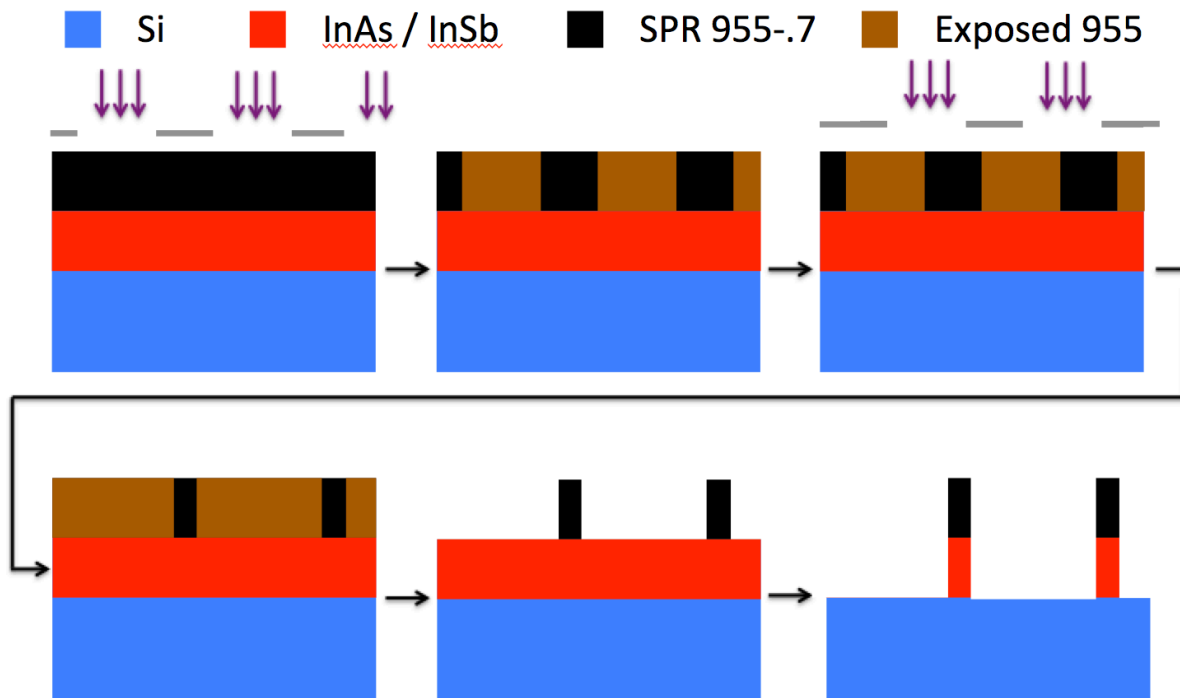


Figure 4. Process cartoon for double exposure using a single resist layer.

width of e.g. 500 nm unexposed and then exposing the same image again with a shift of e.g. 400 nm, should ideally leave a line of only 100 nm fully unexposed, and with positive polarity of the resist, remaining after development. Aside from requiring only a single resist layer and therefore no additional lithography steps, another advantage is that both exposures can be carried out in one ASML run just by the regular stage shifts of the stepper which can be set in 10 nm increments in the job file. So there is no new alignment to the wafer's alignment marks between the exposures which should effectively eliminate the error stemming from that procedure.

To find the smallest linewidth achievable with this strategy, a large number of parameters can be explored and optimized: the exposure dose for 1) the first and 2) the second exposure, 3) the focus offset, 4) the width of the lines on the mask, 5) the shift set in the job file between the two exposures and 6) the reflectivity of the surface which is dependent on the film stack and potential surface treatment. Since fully exploring this parameter space would be prohibitive in terms of time, we followed a sequential approach. The optimum focus offset was determined by a matrix exposure before every ASML run. Initial tests varied the width of the lines on the mask. Intuitively one would assume the best starting point is the narrowest line achievable without double exposure, which is around 350 nm. However we found better repeatability and more consistent results when using 500 nm lines, i.e. when not fully pushing the limits in this regard.

All later testing was therefore done with 500 nm lines. We also decided to not vary the exposure dose between the first and second exposure, and to consistently use one material stack – 50 nm of SiO₂ on blank silicon wafers, in order to not vary the reflective properties of the surface. Potential treatments such as BARC might be explored in the future. Also, for all testing the resist used was SPR 955-.7, which is known to give the best resolution on ASML using regular exposures.

The main optimization was around the exposure dose and the shift – these were varied using a matrix on several wafers. The results are shown in Tables 1 and 2. Overall, there are many dosage-shift combinations that result in the lines not being resolved, i.e. when trying to make lines that are too narrow then they do not come out, as is to be expected. The finest features can be achieved close to that limit, however even along that there are noticeable differences. There are two sweet spots giving the narrowest lines, one around twice half ($2 \times 80 \text{ mJ/cm}^2$) and the other one about twice the full exposure dose ($2 \times 140 \text{ mJ/cm}^2$) for the resist used, which was determined to be around 150 mJ/cm^2 . When moving away from these optimums, the lines first become wider, and then can also exhibit significant sidewall skewedness. An example of the latter, along with the line resulting from the optimum parameters, is shown in Figure 5.

As shown in Table 2, the sweet spots were further examined in more detail with finer-grained exposure matrices. This did not yield any significant improvement in the minimum linewidth, however. It did show, on the other hand, that there seems to be an intermediate stage between fully intact resolved lines and the line not being resolved at all (labeled “barely resolved” in

Exp \ Shift	200 nm	250 nm	300 nm	350 nm	400 nm	450 nm	500 nm
2x 40 mJ							
2x 60 mJ					202-282 (skewed)	132-237 (skewed)	135-167 (skewed)
2x 80 mJ				158 nm	101 nm	not resolved	
2x 100 mJ			116-159 (skewed)	125 nm	not resolved		
2x 120 mJ			121 nm	not resolved			
2x 140 mJ		109 nm	not resolved				
2x 160 mJ		not resolved					

Table 1. Single resist double exposure testing with a coarse matrix varying dose and shift.

Exp \ Shift	340 nm	360 nm	380 nm	400 nm	420 nm	440 nm	460 nm
2x 40 mJ							
2x 50 mJ							
2x 60 mJ							145-289 (skewed)
2x 70 mJ				141-202 (skewed)	135-184 (skewed)	118-150 (skewed)	not resolved
2x 80 mJ					115 nm	98 nm	not resolved
2x 90 mJ				110 nm	115 nm (barely)	not resolved	
2x 100 mJ			barely resolved	barely resolved	not resolved		

Table 2. Single resist double exposure testing with a fine matrix varying dose and shift.

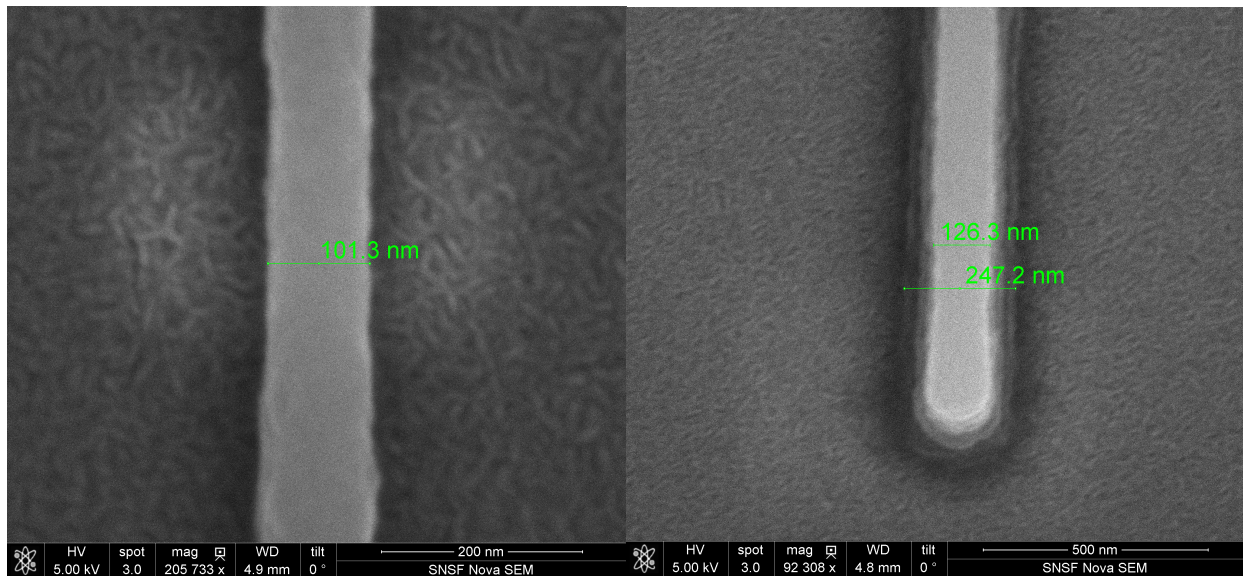


Figure 5. Ideal and highly non-ideal resist profiles resulting from single resist double exposure.

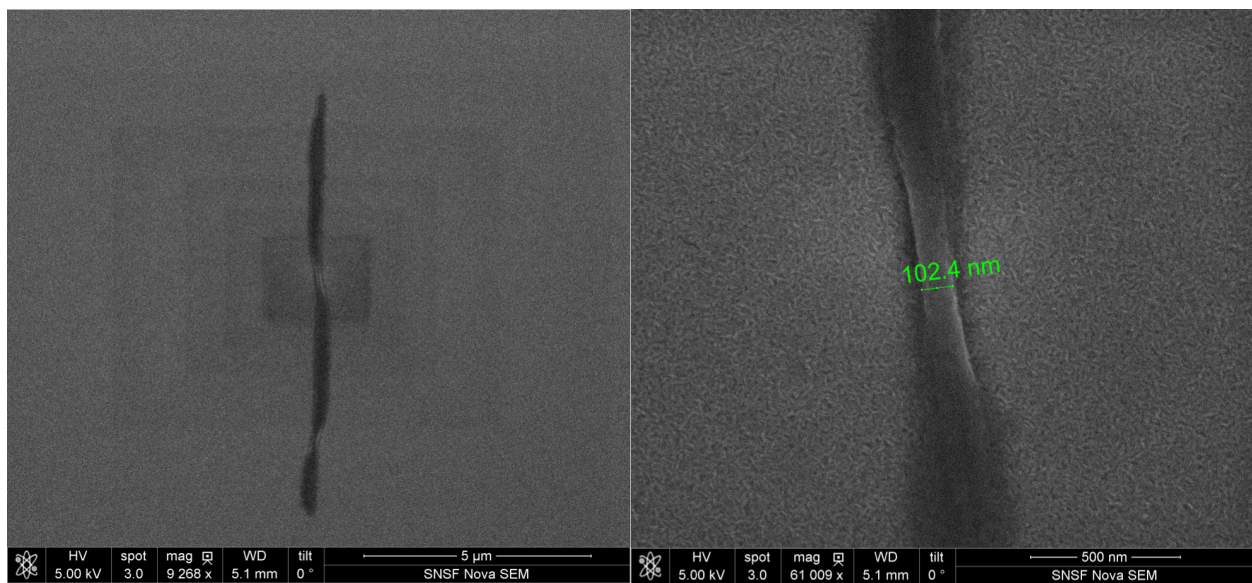


Figure 6. Line of doubly-exposed resist partially fallen over, overview (left) and center (right).

Table 2), where there is still some resist there but much too wide and without sharply defined edges. The SEM images depicted in Figure 6 led us to the conclusion that in most cases this is resist that has fallen over. Figure 6 is a special case in making this clearly visible since the upper part of the resist line has fallen to the left and the lower part to the right. The resist falling over seems very plausible considering the aspect ratio, which at 100 nm width is 7:1, whereas a common rule of thumb suggests not to exceed 3:1.

Assuming that the aspect ratio was indeed the limiting factor for the width, that would mean one could achieve narrower lines by using thinner resist. Therefore two methods were explored to test this. The first was to use a higher spin speed on the svgcoat2 track. This requires minimal

effort and still results in a perfectly uniform coating, however the lowest thickness one can achieve by this is only 500 nm (compared to the default 700 nm). To go lower we also attempted thinning the resist layer before exposure using an O₂ plasma etch in drytek2. This proved non-ideal for several reasons. First, the tool is outside the yellow room leading to a partial exposure. However, by keeping the wafers in one of the blue litho boxes and fast loading and unloading, this can be minimized, resulting in a resist loss (before vs. after development) of only around 30 nm. The bigger issue is the nonuniformity and variability in the tool's etch rate. Due to nonuniformity it is only practical to thin the resist to about half its original thickness, otherwise variations far in excess of 10% are unavoidable.

The above matrix testing was repeated with thinner resist, and it turned out that it was not possible to achieve narrower lines than before, or even noticeably better resolution when not doing a double exposure. The optimum exposure values were very close to the ones for 700 nm thickness, except that the window of the acceptable doses and offsets was significantly narrower for the thinner resist, i.e. it was more unforgiving for values slightly off.

In summary, while the double exposure with single resist was overall successful in giving significantly narrower lines than traditionally possible, at virtually no additional process complexity, with 100 nm linewidth it did not come close in satisfying our 50 nm requirement, leading us to explore further options.

3.2 Hard Mask Double Exposure

Using a hard mask is probably the most well-known way of using double exposures. The process flow for this is illustrated in Figure 7 – a hard mask layer is etched after regular lithography, then the lithography is repeated with a shift, followed by the etch, leaving behind narrower lines of the hard mask material.

As mentioned previously, the lithography tests were done on blank Si wafers with 50 nm of SiO₂, and the latter deposited by PECVD in ccp-dep using the standard recipe at 350 C. The required hard mask etches were done in p5000etch using the standard oxide recipe. Also analogously to before, the main parameters investigated were the exposure dose and the shift.

Unlike for the previous method, a minimum width, below which the lines would not be resolved, was not found. Instead, the only limit for the narrowest lines that are practical is imposed by the line edge roughness, and width variation. As shown in Figure 8, their magnitude becomes very significant for lines below 30 nm, leading to lines below 15 nm being inevitably broken at several points.

The influence of the exposure dose is also much lower than in the previous case, with it mainly just shifting the overall width. For the optimum line edge roughness, it tends to still be optimal to choose a value close to the correct exposure. In that case, it is possible to have lines that are consistently 40 to 50 nm wide and unbroken over several um, as shown in Figure 9.

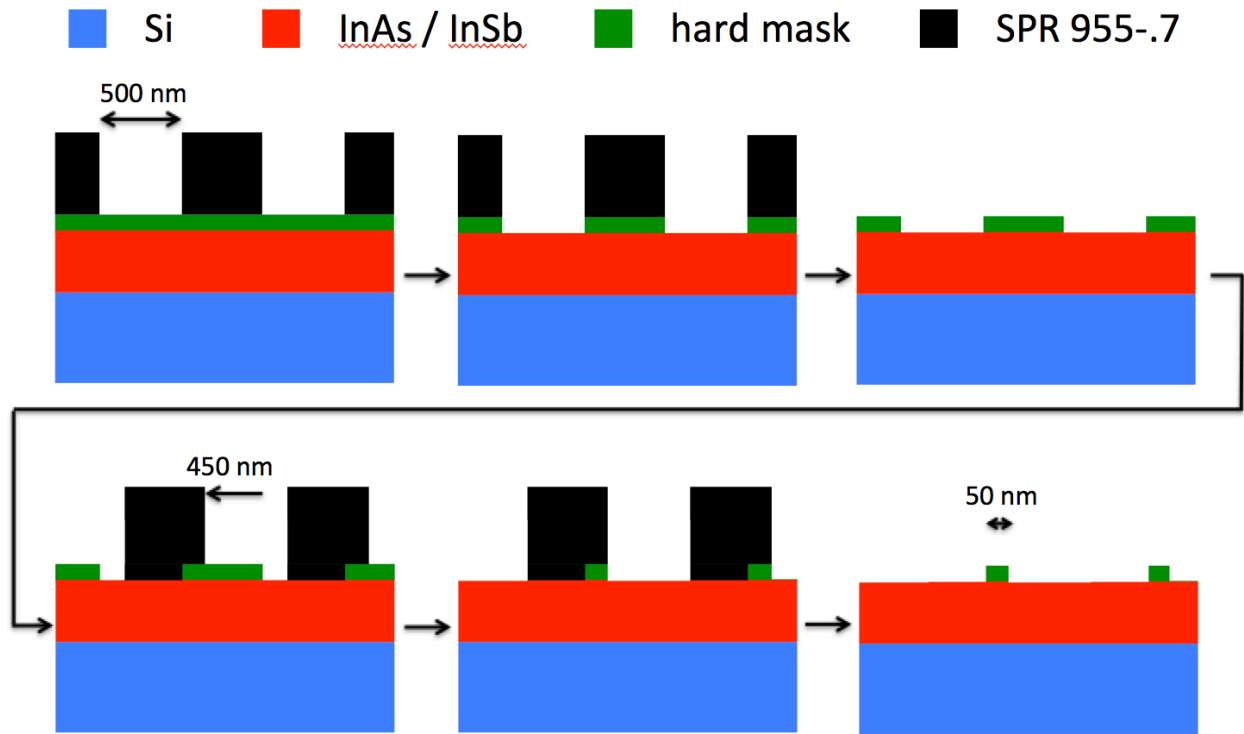


Figure 7. Process cartoon for double exposure using a hard mask and dry etching.

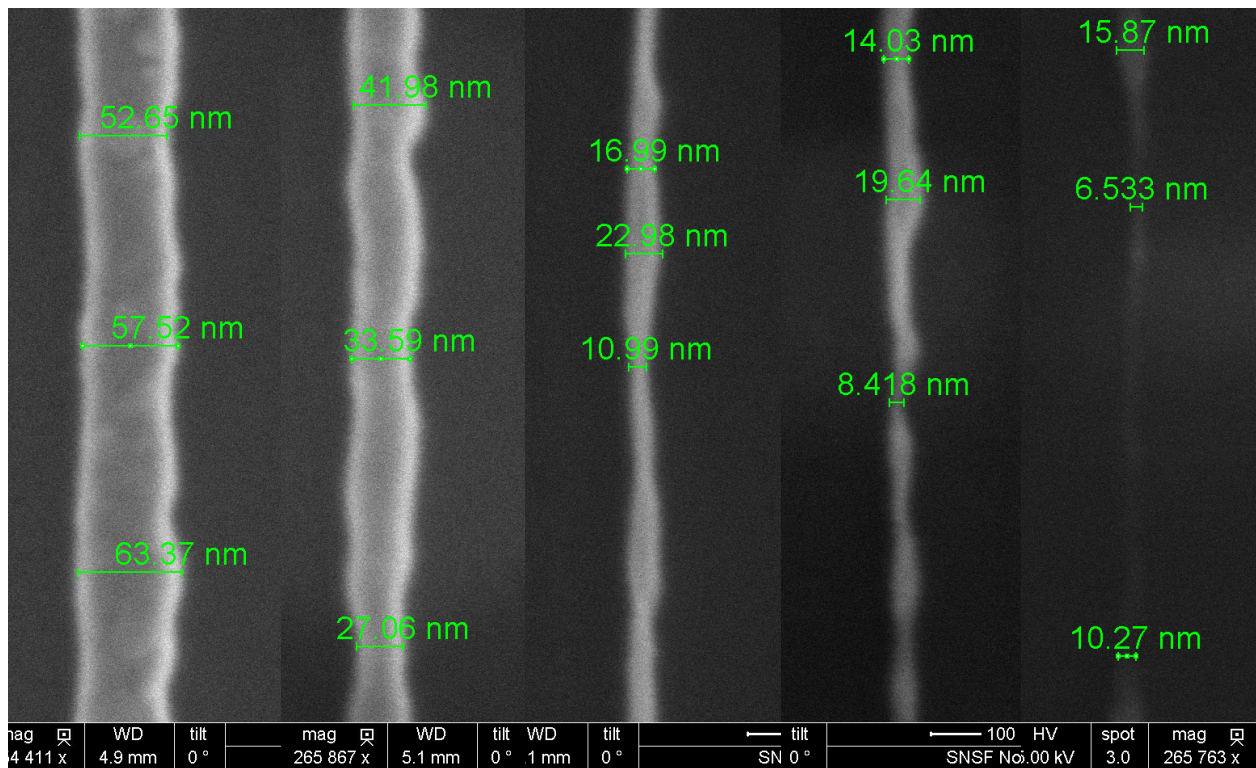


Figure 8. Oxide hard mask line segments after double exposure, for varying shifts.

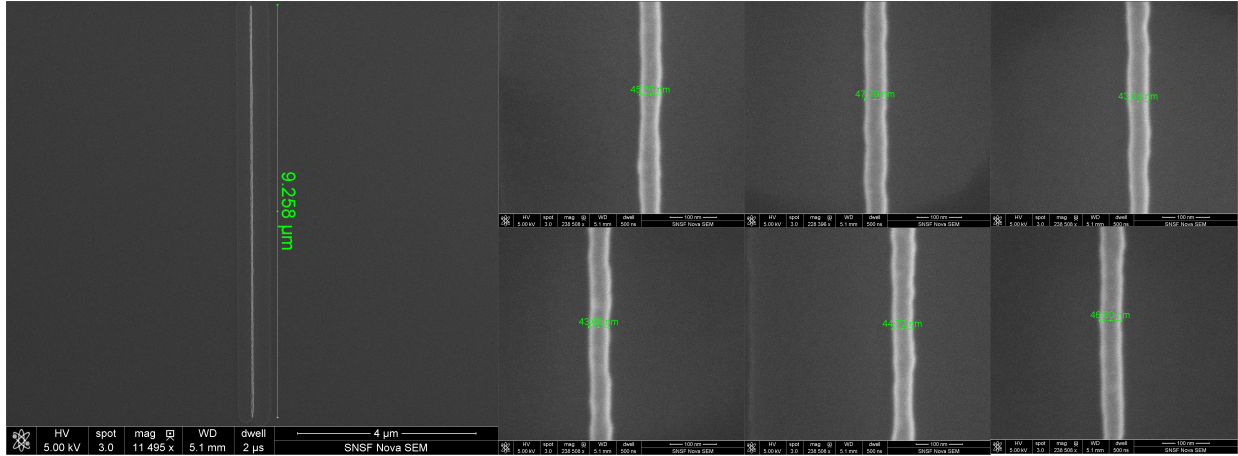


Figure 9. 40-50 nm wide oxide hard mask line segments from 6 different exposure shots (right), with a full view of the bottom right line (left).

A comparison was made between lines from layers 1) deposited in ccp-dep and etched in p5000etch, 2) deposited in ccp-dep and etched in PT-OX, and 3) deposited in thermcoLTO and etched in PT-OX. One hypothesis was that thermcoLTO oxide might result in denser films and therefore less line edge roughness. This could not be confirmed, with a slight tendency towards the opposite; manual interpretation of the SEM suggests that ccp-dep and p5000etch give the best results.

Something that does make a very significant difference, however, is polymer descum in drytek2/4. Leaving this step out not only leads to polymer residue remaining on the wafer, but also higher line edge roughness and width variability (Figure 10). Another source of width variability that cannot be as easily addressed are loading effects: Lines that are at the edge of larger exposed areas, as opposed to in the center, can turn out on the order of 20 nm thicker, however this subsides quickly when moving away from the very edge.

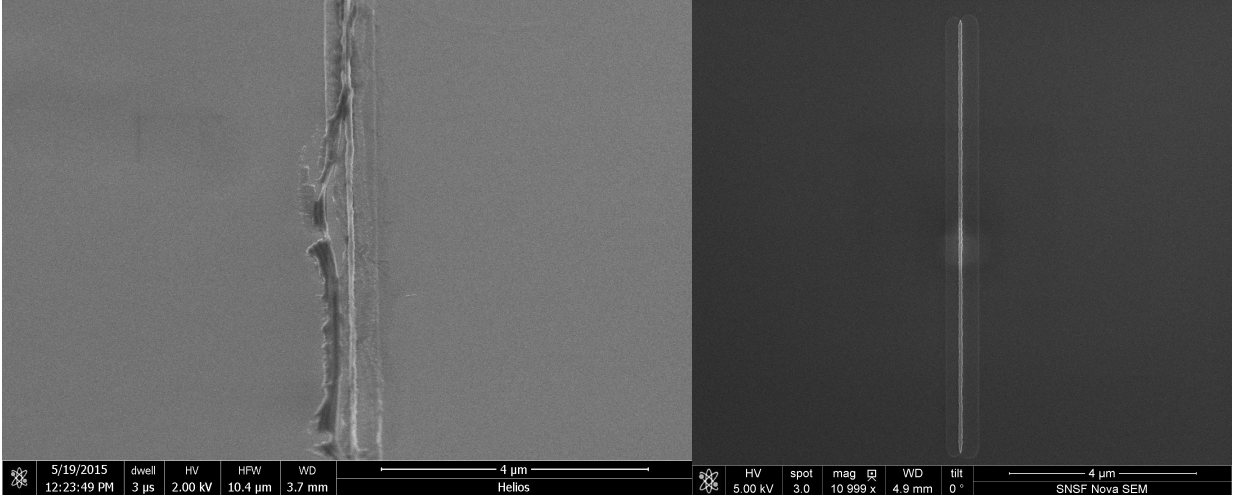


Figure 10. Oxide hard mask lines without (left) and with (right) a polymer descum after etching.

The issue of width variability was investigated further, as it is overall the main challenge associated with the hard mask approach. The variability can differ when comparing between several different hierarchies: One could expect to find different standard deviations of linewidth, 1) within each line, 2) between different lines within the same exposure shot, when comparing the averages for each line, 3) between different shots with the same exposure settings, when comparing the averages for each shot, and 4) between different wafers when comparing the averages over the whole wafer.

In order to eliminate randomness, for each of those hierarchies at least a handful of data points, i.e. SEMs, had to be acquired. To achieve that, 4 wafers were processed in the same batch under identical conditions, and on each wafer 4 different exposure parameter combinations were analyzed (the same parameters on each wafer). For each combination on each wafer, 4 different exposure shots were looked at, and within each shot 4 lines were randomly selected (except for avoiding the edges due to the aforementioned loading effects) and a random portion of the line was imaged. So overall for this purpose a total of $4 \times 4 \times 4 \times 4 = 256$ SEMs were taken, all at magnifications around the same value.

Since manually performing analysis on this many images would be infeasible, Mathematica code was developed that utilizes the software’s image processing capabilities to find the edges of the vertical oxide lines in the SEM images and then calculates the linewidth for each of the 882 rows of pixels in each image (for a total of $882 \times 256 = 225,792$ data points). Correct scaling was ensured by automatically reading in the magnification number from each scalebar using optical character recognition. From the resulting data, estimates for the different standard deviations described above could be calculated, with the results shown in Table 3.

Within each line segment (RMS roughness)	3.0 nm
Between different lines within each shot	3.8 nm
Between different shots with the same exposure parameters	2.7 nm
Between different wafers	16 nm

Table 3. Standard deviations of linewidths for various sets of lines.

From the first three values being essentially the same, one can deduce that within each wafer, the variation between different lines with the same settings, no matter if in the same shot, is on the same order as the variation between several segments of each line. The “stepping” of the ASML and the spacings on the reticle can therefore be assumed to be perfectly accurate.

The same cannot be said, however, for the alignment to each wafer between the two exposures, which is most likely what leads to the significantly higher standard deviation between wafers. This also has practical implications – while it is possible to pattern an ensemble of lines on a wafer that all have close to same width, i.e. within a fairly small range of less than 10 nm (as qualitatively shown in Figure 9 and quantitatively proven by Table 3), the actual location of this range, such as 40-50 nm versus 60-70 nm, is subject to significant variance. Since this deviation

is large enough to probably matter for most applications, when using hard mask double exposures in practice it will likely be necessary to bracket the shifts on each wafer within a range of 30 or 40 nm in 10 nm steps. Then, on each wafer one of the 4 or 5 shift settings will hit the target width. One could therefore say that the price for using this technique is to sacrifice 75-80% of the devices on the wafer as suboptimal. However even accounting for that, the throughput and cost should still be a significant improvement over e-beam.

3. Electron Beam Lithography

Electron beam lithography uses a finely focused beam of electrons to define patterns onto a polymer-coated wafer. This means that it is possible to exceed the patterning capability of optical lithography. Various feats of sub 10 nm features have been realized. This is possible because one can define the beam diameter down to 2 nm. Other reasons to use e-beam are that no physical mask is required as in optical photolithography. This is great for research purposes as it cuts down on cost and results in rapid turn around on design modifications. Also small pieces are a non-issue as there are a variety of cassettes to accommodate a large range of sizes and shapes. It was clear from the beginning that achieving the 50 nm target dimension of the nanoblades for our project would not be a challenge using electron beam lithography.

3.1 Initial tests

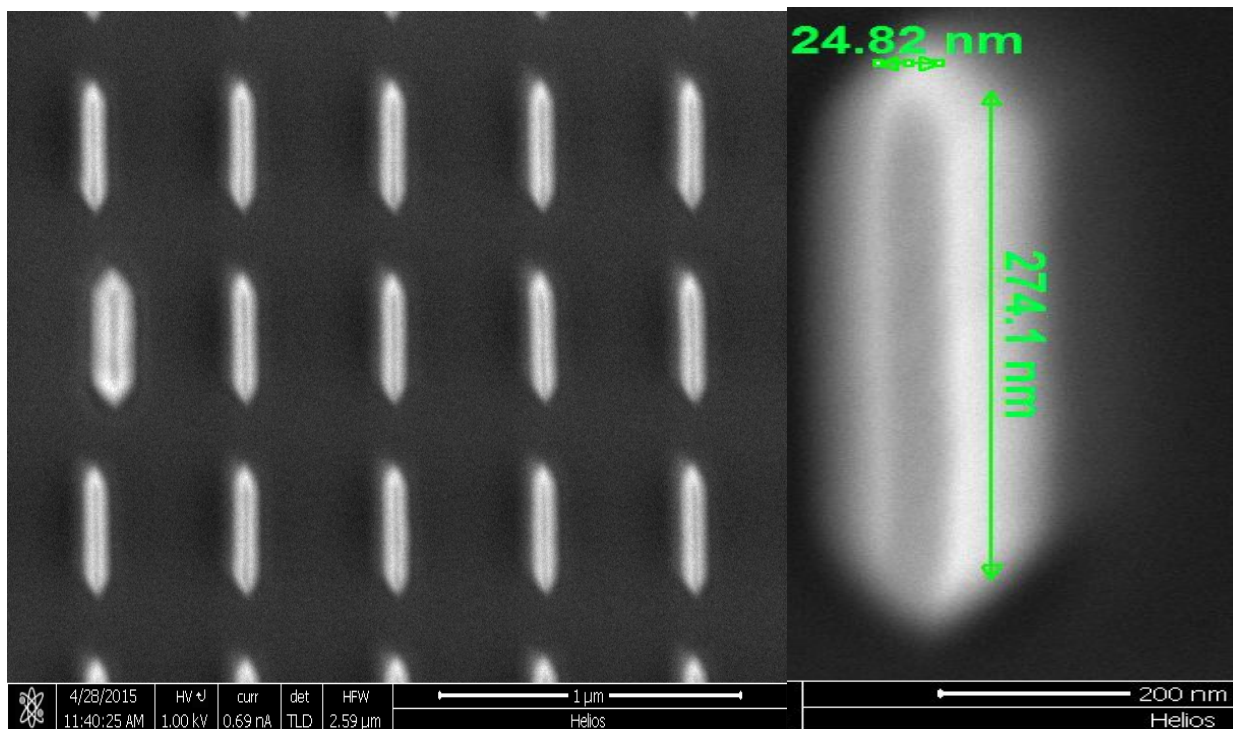


Figure 11. Left: SEM image of an array of 10 by 300 nm nanoblades (target dimension). Right: Magnified image of a single blade with measurements of the actual size.

Prior to making the full structures we intended to make, we wanted to test what limit could be attained with e-beam. We made a simple layout, designed with very small nanoblades, starting from 10 by 100 nm up to 10 by 300 nm. Using MaN 2405 (negative) resist diluted 1:2 in anisole and spun at 4500 rpm gave a thickness of 94 nm. Exposed to a dose of 4000uC/cm². The base dose used was very high, but necessary for features that small. To push the limit even further we could have created nanoblades with zero width in our mask but did not investigate this. The result was that the width of the blades turned out to be in fact between 20-25 nm (see Figure 11). Although this represents a 4:1 aspect ratio, we can see a whole array of them where most of them remained upright, however one has clearly fallen over. This was encouraging, for our required width gives us some breathing room and it is clear that we should not run into issues with trying to get 50 nm linewidths using e-beam.

3.2 Pattern Development

After determining the limit we could achieve with the negative resist, we wanted to pattern longer nanoblades that are closer in dimension to the nanoblades that would be in the devices we would eventually fabricate. Figure 12 shows our mask design. We made nanoblades of differing lengths spanning 1 μm – 20 μm , and widths between 30 – 50 nm. We made 3 by 3 arrays of all of these variations. In addition we added what would look like our final device, a nanoblade

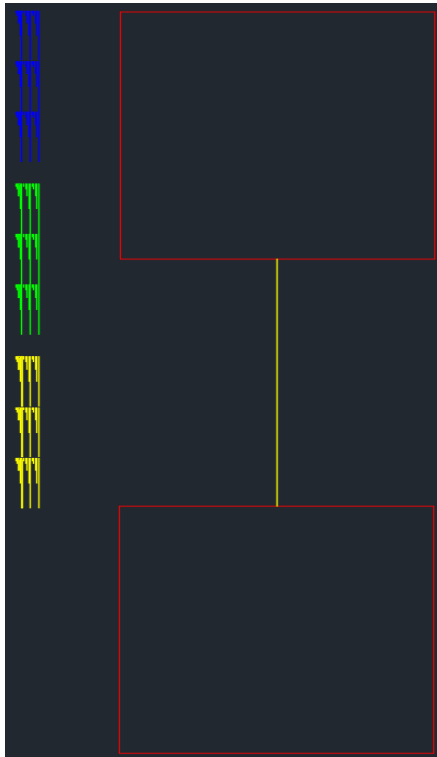


Figure 12. Left: 3 by 3 arrays of free standing nanoblades. Blue – 30 nm width, green – 40 nm width, yellow – 50 nm width. Nanoblades ranged from 1 – 20 μm long. Right: A 100 μm by 50 nm nanoblade anchored by pads on each side having dimensions of 100 by 100 μm .

anchored by pads so that we could make contact and perform electrical measurements. The pads are 100 by 100 μm and the nanoblade in the middle is 100 μm long by 50 nm wide, i.e. very high aspect ratio. The colors in the images have a purpose behind them. Since the dosage required for the different widths is different, it is important to make these features on different layers. Hence everything 30 nm in width is one color, in this case blue. Also for features that are wildly different in dimensions, it is good to leave a decent amount of space between them in order to reduce backscattering of the electron beam, which is caused by the proximity effect. Lastly when importing the design into BEAMER (software that then exports files to JEOL computer), it is wise to make sure it is a GDSII file. Although other formats are compatible with the software it often does not read them correctly.

3.3 Pretreatment effect

Ready with my pattern, we completed an e-beam session after carefully choosing the aperture, current, and trying a whole range of doses. Confident that the pattern would come out the way we expected, we were surprised to see that quite a bit of it did not actually remain on the substrate. Mainly the bigger features remained and only some 50 nm wide lines. Even some of those were wobbly looking (Figure 13). The reason was very poor adhesion between the resist and the substrate. To remedy this, a proprietary chemical known as SURPASS 3000 can make a huge difference. If prior to spinning your resist you use SURPASS 3000, you can get much better results. SURPASS 3000 kills two birds with one stone in that it both cleans the surface of all electrostatic surface contaminants and is also a priming agent, just like HMDS. And not only does it accomplish both of these, it requires a few drops to cover the surface of your wafer and takes only 2 minutes after which you rinse the wafer with water. In addition it is completely non-hazardous, unlike HMDS. So once again after doing this pretreatment, we can see that the adhesion of the resist is much better and that most of the features are intact. The features that didn't come out can be fixed by tweaking the doses a little more but SURPASS solves the adhesion issue.

3.4 Different Resists

As part of the class, we were interested in creating our patterns with both positive and negative resists to characterize how well each stood up against the etching process. For positive resist this meant that we needed to make the inverse pattern. Instead of trying to make the inverse pattern from scratch, you can save a great deal of time by using your existing pattern and doing some simple manipulations on BEAMER software. There one can use a Boolean operation to apply a bias to the design. This effectively creates a border around your existing pattern and the bias is the thickness of this border. So in our case we tried a bias of 100 nm around our nanoblades (Figure 14). Of course to isolate the features from all the resist that would remain it would be wise to space out the pattern more and apply a bigger bias. We did a selective bias of our pad when we tested out PMMA A4 resist, applying a bias of 5 μm around it so that it would be moderately isolated. In order to do a meaningful test we planned on using four different resists,

MaN2405 (negative resist), which was already shown earlier in the report, PMMA A4 (positive resist), Zep 520A (positive resist), and HSQ (negative resist). Thus with two positive and two negative resists, we could see which one of each tone was more suitable to hold up not only against the ebeam, but the etching process as well.

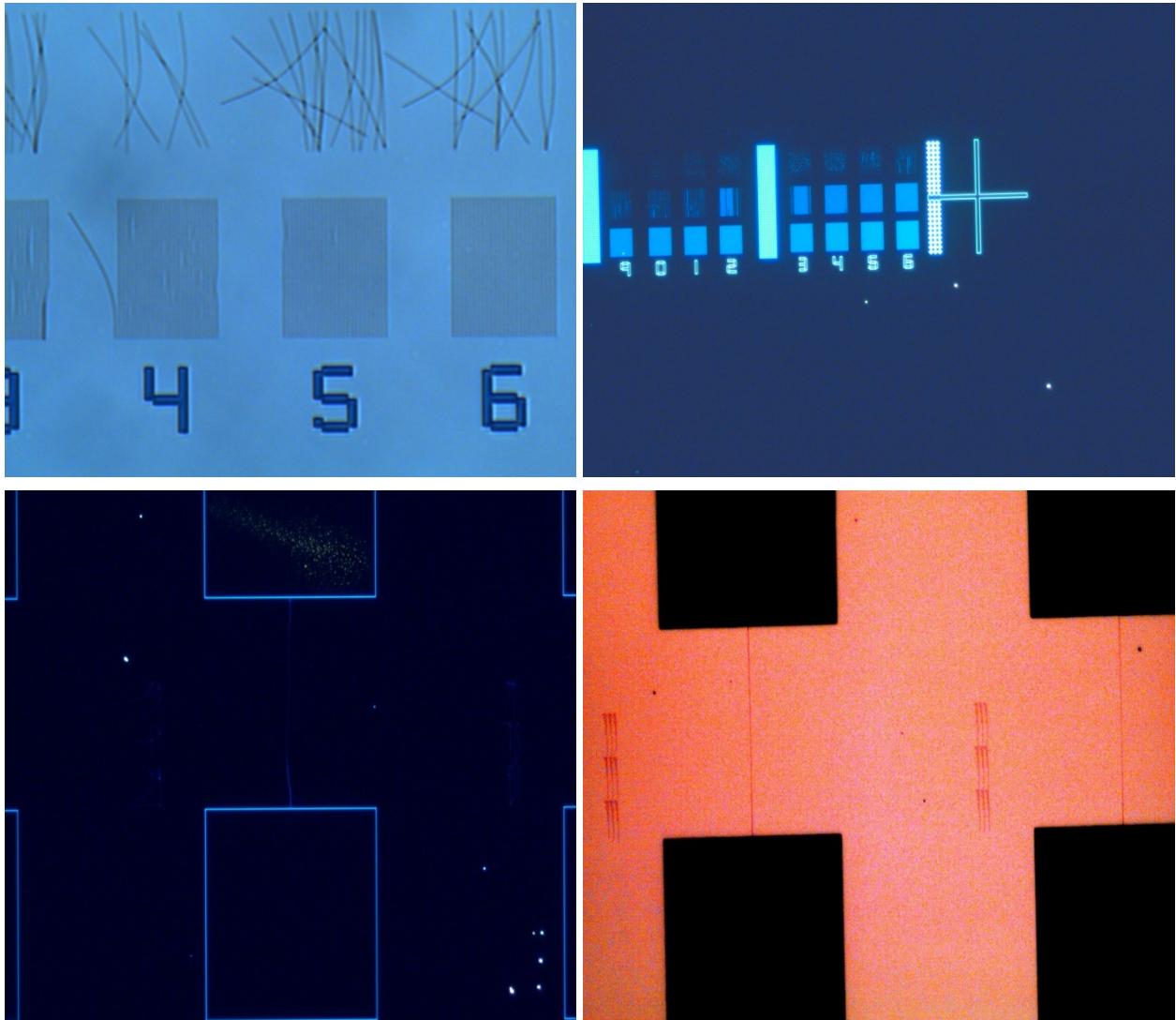


Figure 13. The two images on the left are the result of no pretreatment done. The narrower nanoblades in the top left hardly remained on the surface and those that managed to do so were disheveled. Bottom left: The pads are clearly visible in dark field image, but straddling nanoblade is tilted and only partially intact. Free standing nanoblades to the left of the device structure are wholly missing. Images on right had SURPASS 3000 pretreatment. There, the nanoblades are mostly intact except for the smallest ones in the top row. That can be fixed by correcting the dose. Bottom right: The nanoblades are visible both free standing and the one present between two pads is perfectly straight.

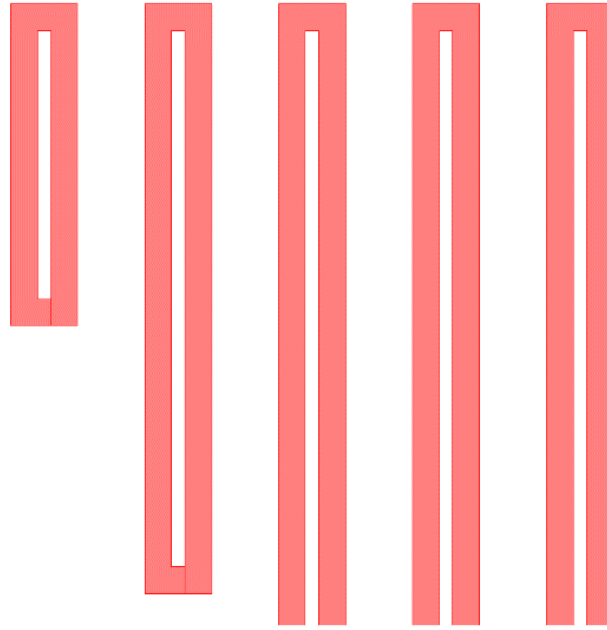


Figure 14. Illustration of biasing around the nanoblades to invert the polarity of the layout.

Resist	Tone	Dilution	Pre-Bake Temperature	Bake Time	Developer
Zep 520 A	+	1:2 Anisole	70 C	30 s	MIBK:IPA (1:1)
PMMA	+	-	180 C	90 s	MIBK:IPA (1:3)
HSQ	-	-	80 C	60 s	MF 319
MaN-2405	-	1:2 Anisole	90 C	45 s	MF 319

Table 4. Properties and suggested conditions for the resists used.

Table 4 lists the different resists utilized and some of the conditions we used that can be used as a starting point for your own work. Note that HSQ is not available in SNC and is very expensive (\$6/mL). We further characterized the thickness of the resist using Filmetrics (in SNC), which is a spectral reflectance based method – a very quick and contact-less approach to get an estimate of the thickness of your resist. We obtained the values shown in Figure 15 for each of the resists when using recipe 8 in the spin coater, which was 5 seconds of 505 rpm followed by 40 seconds 4500 rpm. This was the fastest spin recipe already programmed. We did this to get as thin a resist layer as possible in order to limit forward scattering, which can be mitigated by limiting resist thickness or increasing the accelerating voltage. It also means the dosage required can be lessened a bit as well.

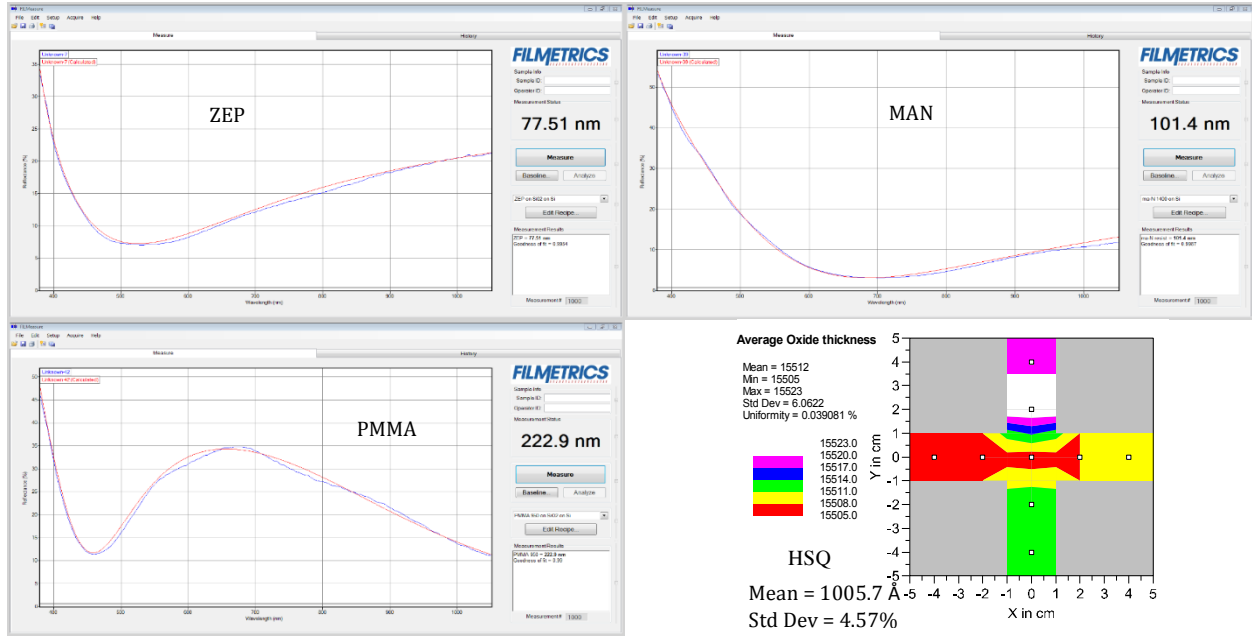


Figure 15. Thicknesses of different resists measured using Filmetrics. Bottom right: HSQ thickness was measured on woollam in SNF. All resist were spun at 4500 rpm.

3.5 Determining appropriate dosage

There is a very simple equation $D = (I \cdot t) / A$, where $D = \text{dose} [\mu\text{C}/\text{cm}^2]$, $I = \text{current} [\text{A}]$, $t = \text{time} [\text{sec}]$ and $A = \text{exposure area} [\text{cm}^2]$, that one uses to determine how long their patterns will take and what dosages are required. The right dosage will ultimately depend on the size of your features and the resist you use (thickness and composition). We found that for the patterns we were interested in, 200-400 $\mu\text{C}/\text{cm}^2$ as a minimum base dose got the job done for Zep 520A, PMMA A4 and MaN-2405. In the case of HSQ (also known as spin-on glass) a base dose of at least 1000 $\mu\text{C}/\text{cm}^2$ worked well. Of course when you first start out, you want to try a large range of doses and see which one comes out best and then hone in around that value for your subsequent runs. Lastly based on the time it would take and the features you have you would accordingly choose the correct aperture and beam current to get the minimum base dose you are aiming for. In general the smaller the pattern and the more isolated the pattern, the higher base dose is required.

3.6 Optical images of different resists with same patterns

In Figure 16 we see the results under an optical microscope with a camera in SNC. The colors are all false but necessary to see anything at all. This was done by increasing the contrast to its maximum and adjusting the brightness until something was visible. Starting with the left side, we see that all the features showed up and slightly isolated, as we had only a 75 nm bias around our

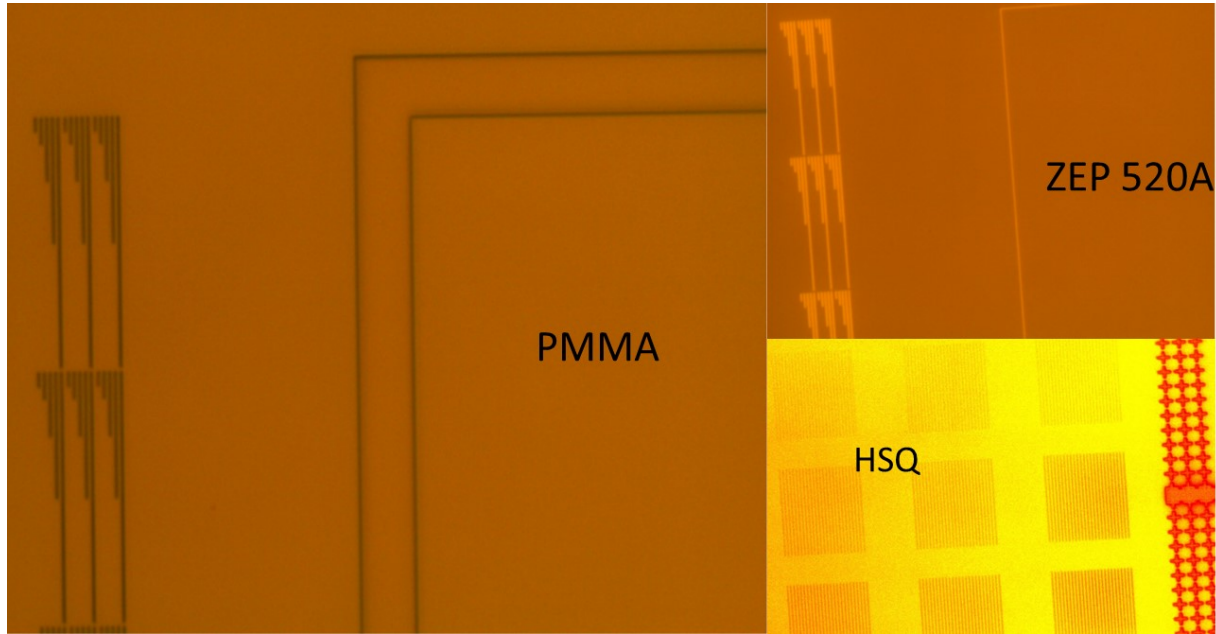


Figure 16. Comparison of different resists with similar patterns using an optical microscope.

free standing nanoblades. We are unable to resolve the actual nanoblades, which are only 30 nm in width and would require an electron microscope to visualize. The big pad has a bias of 5 um around it so that it would be sufficiently isolated from the surrounding resist. We do know that the dosage was correct because everything shows up and is straight. On the top right is the run we did with Zep 520A which shows that our isolated nanoblades are not actually isolated. We had applied a bias of 200 nm for all features. Thus we see that the blades are all touching and the big pad to its right is hardly isolated from the surrounding resist. The last resist I tried was HSQ (negative tone) which also shows that all features appear. The features in this image are just free standing nanoblades. Here we had patterned 50 nm by 10 micron blades in the last row and the two rows above show 40 and 30 nm by 10 um blades in that order.

3.7 Electron Beam Lithography Manual

The purpose of this manual is to get you confident enough to run the Ebeam yourself after a single training.

This will be done in the order in which you should be working on each step in order to maximize efficiency.

- 1) Clean your wafer with ozone for 5 min (if ozone is not detrimental to your process). This will get rid of organics that may be present.
- 2) Set hot plate to desired temperature (used for pre-bake).
- 3) Use SURPASS 3000 on your wafer to get rid of electrostatic contaminants and leave behind cationic monolayer with which to receive the resist. To do this, take a shallow glass plate and place wafer down. With a pipette spread some SURPASS just to cover the

entire surface – the surface tension keeps the liquid as a puddle on your wafer. Let sit for two minutes and rinse with water.

- 4) Spin your resist, positive or negative. To operate spin coater place correct holder depending on wafer size and press Vacuum ON. With a pipette deliver volume of resist to cover 80% of the surface and without delay start desired recipe.
- 5) Place on hot plate for time indicated by your recipe.
- 6) Load your sample in the Ebeam cassette. Choose the size and direction of the cassette appropriately. The wafer piece needs to at least cover all the empty space between the copper plates. The schematic on the wall shows which compartment you are using, (eg E, F, G, H, etc). Place samples face down and near central mark. Record the workable dimensions of your wafer piece and dimensions of cassette.
- 7) To load your wafer into the holder, vent the chamber by rotating lever clockwise and pressing vent. Unload the holder and place the cassette face up (you should see your resist coated wafer). Slide it in and with the air gun blow the bottom so no lint is present. Place the holder back in chamber and make sure that the receiving handle is situated between the two prongs. These prongs are going to deliver the cassette into the main chamber.
- 8) Shut the chamber and rotate level counterclockwise and press vent (same button for venting and pumping).
- 9) While you wait for it to pump down, go over to the computer and import your pattern (which is in GDSII format) into BEAMER software. After making sure in viewer mode (hit play button next to imported file) that it is the way you made it, export the file, which you will save as a work flow folder (.ftxt file). This will have created a (.v30 file, which you should write down (limited to 20 characters)) which you can transfer to JEOL computer.
- 10) To transfer this file go to SECUREFX – Jeol – pattern – user – RISSMAN. Now drag your .v30 file(s) over there.
- 11) Now enable the instrument on Badger.
- 12) On left computer, press source and when prompted type in Jeoleb (test will not appear). Press enter to log in.
- 13) Click on main only tab in bottom of right monitor.
- 14) Click CLB – EOSSET (choose aperture and current settings) by choosing the file and executing and saving and then hit cancel to exit.
- 15) Next click Current, execute, which reads out current. Click save and cancel.
- 16) Click HHEIMAP (reads height of wafers automatically, thank god for that). Lets you know variation in height of how wafer is sitting and positions. Choose appropriate slot (e.g. 2E, etc.). Choose the number of points at which it will measure at, typically set to 5 by 5 but can be changed. The goal of this is to make sure you understand where your wafer is sitting. Based on the dimensions of your wafer you can change the distances between each measurement. Click Save and cancel.

- 17) Click on EDIT JOB 1 in bottom of right monitor (this is where text editing takes place).
- 18) Open file cabinet icon – job – user – open sdf (standard data file) in left window, jdf (job deck file) in right window and expand to full screen, and open terminal (fortran script) in left window.
- 19) Save the sdf file as new name and change the date, save jdf file as the same new name and save the file. Continuously save as you make changes.
- 20) In terminal, type bash – enter.
- 21) Next type ls (which lists the files you have).
- 22) Next type schd (filename.sdf) – enter (If everything was done correctly it makes a magazine file with no error).
- 23) In sdf file in the top left, specify position (2E, 2F, etc).
- 24) Remove the semicolon from the current an aperture setting you plan on using.
- 25) Minimum base dose determined by equation $(4000 * I(nA)) / (\text{step size (nm)})^2$
- 26) Near the bottom of the page, there is a line with the minimum base dose ($\mu\text{C}/\text{cm}^2$), the current in uC per line, L. This can be modified accordingly
- 27) Make sure to call correct .jdf file within the .sdf file.
- 28) Edit .jdf file by first modifying the array, where is that you will physically pattern on your wafer (this is why knowing dimensions of your wafer is useful). In ARRAY CHECK tab in right monitor at bottom click on it and this allows you to see where the pattern will be in space. Open magazine file you generated. Each time you update click reset to see modifications you made.
- 29) After being satisfied with the where your full pattern will repeat, assign where the patterns will be in x and y space.
- 30) Define your pattern by writing down the file (.v30 file you made)
- 31) Next define the dosage by calling it a certain name (6 characters only) and typing in MODULAT followed by (pattern number, % increase from base dose). A negative number is a decrease in base dose, while 0 is the base dose.
- 32) SAVE this final version creating the final magazine file.
- 33) Go to MAIN TAB – COMMANDS- BATCH – choose file (typically med exposure, if short on time do the short one). Execute and save.
- 34) Mode tab – display mode.
- 35) EBX – EXPOSE – file – magazine file – execute – yes.
- 36) Within expose window – click on CHIP ARRAY DIAGRAM to see how much of the job is done in real time.
- 37) Once writing is done, acknowledge box that says no writing errors and wait for stage to move back to home position of roughly 100 by 100.
- 38) Log out of BADGER
- 39) Remove our sample by opening gate valve and pulling it out. Vent to atmosphere, remove cassette, and place holder back in and pump down.

4. InSb Reactive Ion Etching

4.1 Process Selection

In order to make a final device, vertical InSb blades with a high aspect ratio need to be etched. There are two chemistries reported in literature for etching In-based compounds: $\text{BCl}_3/\text{Cl}_2/\text{Ar}$ and $\text{CH}_4/\text{H}_2/\text{Ar}$. A comparison of these two processes is shown in Table 5. Based on the availability of etch gases on the Ox-35 etcher, either process could have been chosen as the etching process. However, since the evaporation temperature of the volatile product of $\text{BCl}_3/\text{Cl}_2/\text{Ar}$ is high compared to the default chuck temperature (20°C), there is a risk of the plasma electrode shorting. Therefore, the $\text{CH}_4/\text{H}_2/\text{Ar}$ process was chosen as our etching process. For our requirement, the angle of the etched sidewall needed to be exactly 90 degrees. In literature, for both processes only sloped walls and high surface roughness were reported.

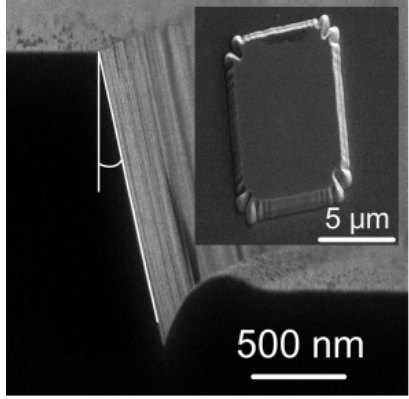
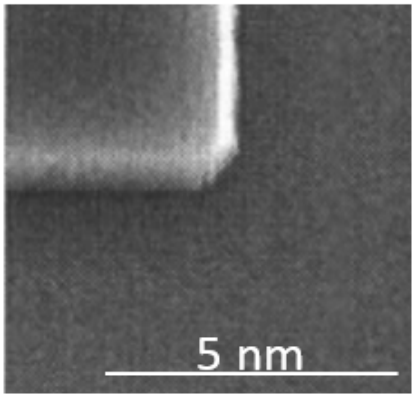
Process	$\text{BCl}_3/\text{Cl}_2/\text{Ar}$	$\text{CH}_4/\text{H}_2/\text{Ar}$
Volatile Product	$\text{InCl}_x (>250^\circ\text{C})$	$\text{SbH}_3 (> -19^\circ\text{C})$
Sidewall profile	Sloped	Sloped, barreled
Roughness (RMS)	~ 33 (nm)	~ 40 (nm)
SEM images from literature		

Table 5. Comparison between $\text{BCl}_3/\text{Cl}_2/\text{Ar}$ and $\text{CH}_4/\text{H}_2/\text{Ar}$ etch chemistries based on literature research.

2. Design of Experiment

Based on the values reported in literature and on our initial experimental results, the conditions and variables listed in Table 6 were chosen for the final DOE parameter sets using JMP. The samples were etched for 3 minutes. The Results are shown in Table 7. Roughness was measured with AFM, and the angle, etch rate, and selectivity were measured via cross-sectional SEM.

	Conditions
Mask Material	Photoresist (SPR955-.7) mask
Substrate Temperature	20 °C
ICP power	600W
RF power	100W
Chamber Pressure	20 mTorr
Variables	1. CH ₄ flowrate (15 – 45 sccm) 2. H ₂ flowrate (4 – 10 sccm) 3. Ar flow (40 – 80 sccm)

Table 6. Selected etching conditions.

Sample #	Factor			Results			
	CH ₄ flow (sccm)	H ₂ flow (sccm)	Ar flow (sccm)	Roughness (nm)	Angle (deg)	InSb Etch rate (nm/min)	Selectivity
1	+	+	+	18.4	60	57.6	1.56
2	+	+	-	31.6	90	75	37.48
3	+	-	+	23.4	90	76.3	2.16
4	+	-	-	32.4	72	74.7	1.81
5	-	+	+	27.6	74.3	57.6	0.99
6	-	+	-	26.8	70.2	69.1	1.34
7	-	-	+	20.2	72.2	62.2	0.97
8	-	-	-	32	75.5	55.4	0.86
9	0	0	0	27.1	90	55.7	1.02

Table 7. Results for final JMP.

4.3 Results and discussion

As shown in Table 3, there is no apparent direct relationship between different parameters and the JMP program did not give an accurate optimal point. The condition for sample 3 (CH₄:H₂:Ar=45:4:80) was chosen as the condition for further experiments with the etching process because of its good selectivity and straight sidewall angle. All etches in Section 4.3 were done with the sample 3 condition.

4.3.1. Selectivity vs. InSb etch rate

An equation between the selectivity and InSb etch rate was fitted. (Fig.1) The equation is as follows:

$$\text{InSb etch rate} = 24.2 \ln(\text{Selectivity}) + 59.3$$

There are a few outliers in the data, but outlier points all have higher selectivity than the fitted line so the equation is a good initial estimate of how thick the photoresist is.

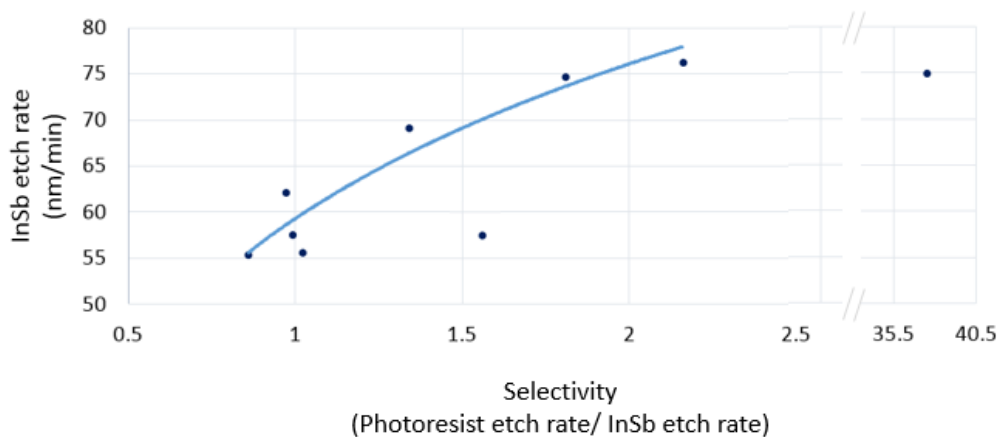


Figure 17. Regression of selectivity and InSb etch rate.

4.3.2 Etching Mechanism

As listed in Table 7, all JMP samples showed very significant surface roughness, for initially unknown reasons. When increasing the etch time, the surface roughness became even worse, resulting in InSb nanowires after 6 minutes of etching, as shown in Figure 18. We developed a hypothesis attempting to explain these observations:

Overall, the problem is surface passivation with $\text{In}(\text{CH}_3)_3$ during the etching process. When the plasma is ignited, $\text{CH}_4/\text{H}_2/\text{Ar}$ plasma generates some hydrocarbon ions and hydrogen ions. H^+ reacts with Sb and forms SbH_3 , which evaporates due to its -19°C boiling point (Table 5). However, In reacts with C_xH_y and forms $\text{In}(\text{CH}_3)_3$, which remains on the surface, because its sublimation temperature is 50°C . $\text{In}(\text{CH}_3)_3$ is then nonuniformly physically etched by Ar. When Sb is exposed after Ar etching in certain areas, Sb is chemically etched by H^+ and the process repeats. Initially, this leads to a gradual buildup of surface roughness. Once the sharp tips of nanowires have formed, they are much less susceptible to the directional physical etching by Ar. The body of the nanowires, parallel to the incident Ar ions, cannot get physically etched either, which overall leads to the nanowires being unaffected by the continuing etch process.

To verify our hypothesis, we did further analysis using XPS on etched and as-deposited samples. The resulting data is shown in Figure 20. When InSb is first deposited, the In to Sb ratio is approximately 1:1. After etching for 6 minutes, however, there is no Sb on the surface. Only In and C are found. When etched with the Ar gun of the XPS tool (2kV, 1uA, 2mm x 2mm) for 0.1 minutes, Sb does appear on the surface again. (The aluminum peak in the XPS is from the aluminum paste used during SEM imaging.) This seems to confirm the hypothesis that the InSb nanowires were grown due to AN imbalance between the chemical etching and physical etching.

This also explains why the data points in Table 3 are random; more than three factors affect the etching process. Also, the reason sample 3's roughness and side wall angle were good is that there was a reasonable balance between the chemical and physical etching up to 3 minutes. Figure 21 shows two different etches done under the same condition except for the ICP power. The higher 1000 W power showed a slower etch rate which was counterintuitive. However, this can also be explained by the imbalance between the chemical and physical etching.

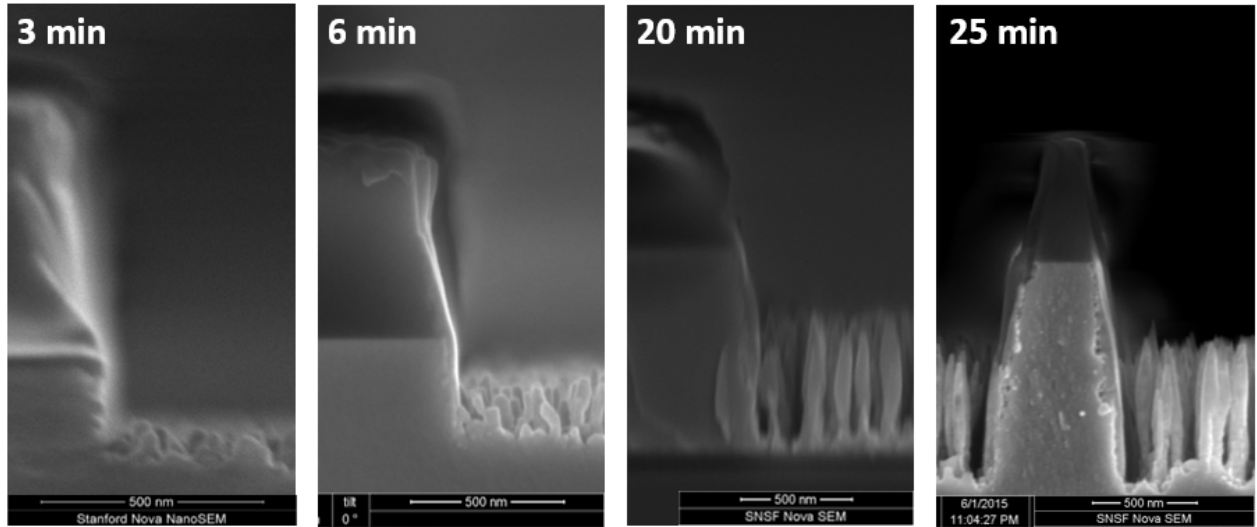


Figure 18. Surface morphology relative to the etching time using sample 3 parameters.

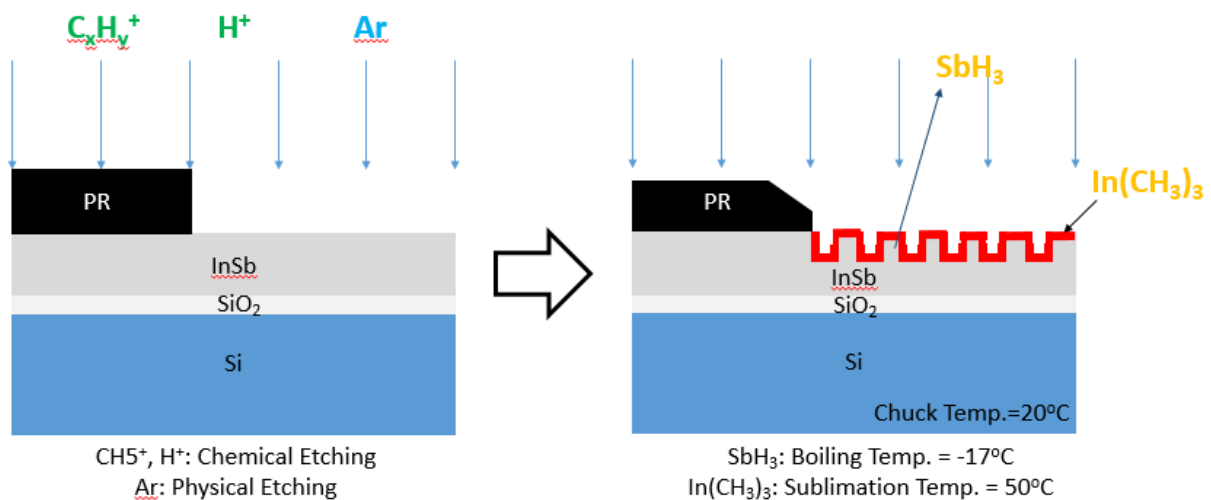


Figure 19. InSb etching process with $\text{In}(\text{CH}_3)_3$ passivation leading to roughness.

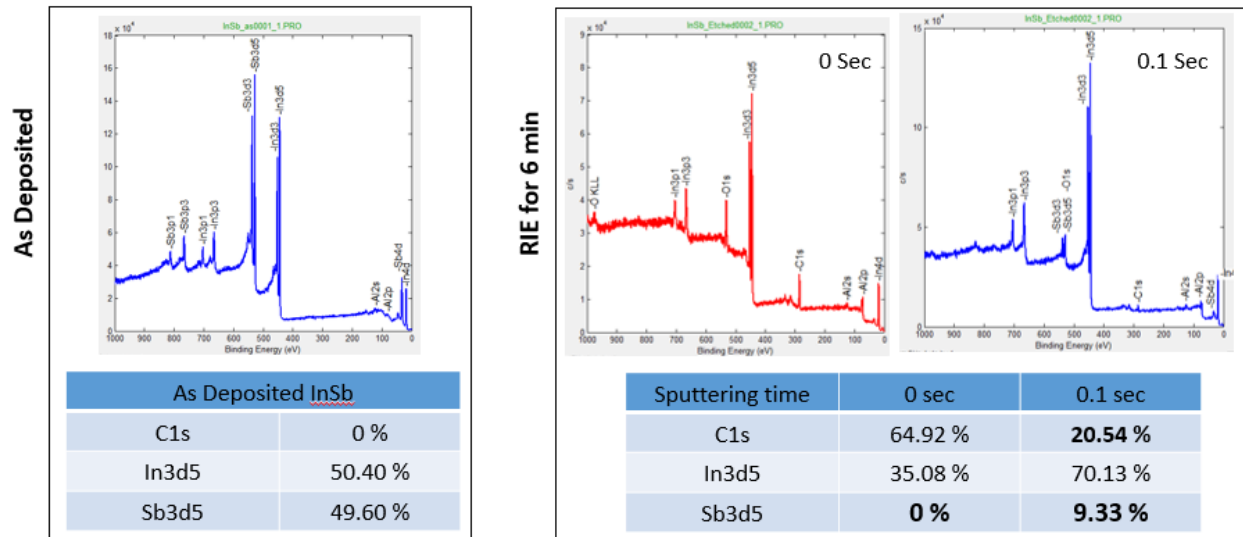


Figure 20. XPS data for as-deposited InSb and 6-minute-etched InSb.

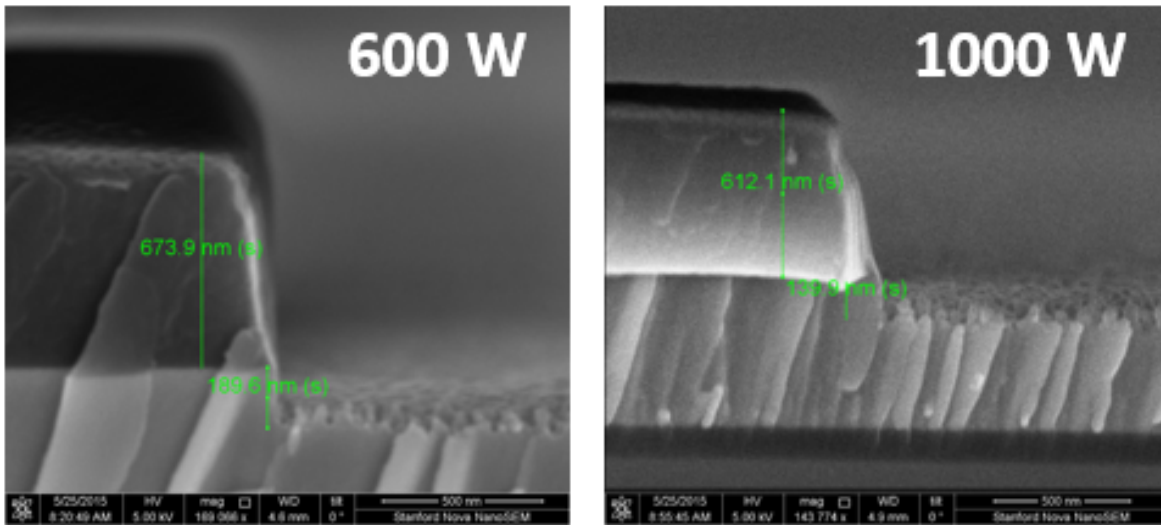


Figure 21. InSb etch profile comparison between 600 W and 1000 W ICP power.

4.4. Future Work

To fabricate a smooth surface and straight wall, the following procedure is proposed. If it is possible to heat the substrate, heating the chuck to higher than 50°C would be helpful in terms of increasing chemical etching of $\text{In}(\text{CH}_3)_3$. If this is not possible, fine tuning of etching conditions should be done to balance between chemical etching and physical etching to find the optimum point for etching.